Towards Workspace Analysis of Platforms with Three Arbitrary Legs

M. John D. HAYES [1] *Manfred L. HUSTY* [2] *Paul J. ZSOMBOR-MURRAY* [3]

[1] Institut für Automtion, University of Leoben, Peter-Tunner-Str. 27, A-8700 Leoben, Austria
[2] Inst. f. Tech. Math., Geometrie und Bauinformatik, University of Innsbruck, Innsbruck, Austria
[3] Centre for Intelligent Machines, McGill University, Montréal, Québec, Canada.

1. GENERAL PLANAR THREE-LEGGED PLATFORMS

In this paper kinematic mapping is used for the workspace analysis of a sub-class of planar three-legged platform. We are working towards using kinematic mapping to develop a procedure which can be applied to the workspace problem of arbitrary three-legged architecture. Such a *general planar three-legged platform* (GP3LP) consists of a moving platform connected to a fixed base by three kinematic chains. Each chain is connected by three independent one degree-of-freedom (DOF) joints, one of which is active, see [2]. From a geometric perspective a GP3LP consists of three arbitrary points F_A, F_B, and F_C in a fixed base reference frame, Σ, and three arbitrary points M_A, M_B, and M_C in a moving platform reference frame, E, with each platform point a specific distance from each base point (see Fig. 1). These distances are determined by the variable joint input parameters and the particular topology of each of the three kinematic chains [4, 2].

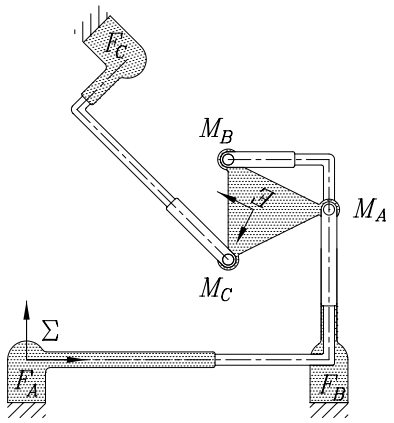

Figure 1. A $P\underline{P}R$-type platform.

In this paper we will deal only with lower kinematic pair joints. Since the displacements of the platform are confined to the plane, only *revolute* (R) and *prismatic* (P) pairs are considered. To construct a leg, there are 7, i.e. (2^3-1), possibilities. The PPP are excluded because three P-pairs represent three translations in the plane, which can not be independent [4]. Since any of the three joints in any of the seven characteristic chains may be the active one, there are twenty-one possibilities for each leg. When the active joint is locked, the resulting two-jointed characteristic passive sub-chain is one of four types. Legs possessing PP-type architecture must be rejected as not useful [4], leaving eighteen possibilities per leg. If leg types can be counted more than once, the possible combinations gives the total number of GP3LP:

$$C(n,r) = \frac{(n+r-1)!}{r!(n-1)!} \quad (1)$$

$$C(18,3) = 1140. \quad (2)$$

The method presented in this paper can be applied to some PR-type architecturally symmetric platforms, in particular, the $P\underline{P}R$-type (the *underscore* indicates the active joint). One similar to that analysed herein is shown in Fig. 1.

2. KINEMATIC MAPPING

A general displacement of one rigid-body with respect to another in the plane can be conveniently described as the relative displacement of two coordinate reference frames Σ and E. Without loss in generality, Σ may be considered as fixed while E is free to move. The image point of a displacement of E in Σ is given by [1]

$$(X_1 : X_2 : X_3 : X_4) = (a\sin(\phi/2) - b\cos(\phi/2) : a\cos(\phi/2) + b\sin(\phi/2) : 2\sin(\phi/2) : 2\cos(\phi/2)), \quad (3)$$

where (a, b) are the coordinates of the origin of frame E in Σ, and ϕ is the orientation of E in Σ.

Using Eq. (3) we can transform the coordinates of a point $(x : y : z)$ in E to those of the same point $(X : Y : Z)$ in Σ:

$$\begin{aligned} X &= (X_4^2 - X_3^2)x - 2X_3X_4y + 2(X_1X_3 + X_2X_4)z \\ Y &= 2X_3X_4x + (X_4^2 - X_3^2)y + 2(X_2X_3 - X_1X_4)z \\ Z &= (X_4^2 + X_3^2)z. \end{aligned} \quad (4)$$

For the kinematic analysis, it is useful to consider an individual $P\underline{P}R$ leg, together with the moving platform, when the platform connections to the remaining legs have been severed. Now, consider the motion of a fixed point in E that is constrained to move on a fixed circle in Σ,

$$K_0(X^2 + Y^2) - 2K_1XZ - 2K_2YZ + K_3Z^2 = 0, \quad (5)$$

where $[K_0 : K_1 : K_2 : K_3]$ are the *circle coordinates*, with $K_1 = X_c$, $K_2 = Y_c$, $K_3 = X_c^2 + Y_c^2 - r^2$, with X_c and Y_c being the coordinates of the circle centre of radius r, and K_0 is an arbitrary homogenising constant. If $K_0 = 0$ we obtain a line, which is a real degenerate circle, with *line coordinates* determined by the relation $[L_1 : L_2 : L_3] = [-2K_1 : -2K_2 : K_3]$. The circle coordinates become:

$$\begin{aligned} K_1 &= \frac{1}{2}F_{i_{z/\Sigma}}\sin\iota_{1/\Sigma}, \quad K_2 = -\frac{1}{2}F_{i_{z/\Sigma}}\cos\iota_{1/\Sigma} \\ K_3 &= (F_{i_{x/\Sigma}} + d_{2_i}\cos\iota_{2/\Sigma})\sin\iota_{1/\Sigma} - \\ &\quad (F_{i_{y/\Sigma}} + d_{2_i}\sin\iota_{2/\Sigma})\cos\iota_{1/\Sigma}, \end{aligned} \quad (6)$$

with i for leg $i \in \{A, B, C\}$, ι for corresponding joint angle $\iota \in \{\alpha, \beta, \gamma\}$ and $/\Sigma$ indicating *with respect to* Σ. The length of the active P-pair is given by d_{2_i}. We use this relation rather the standard form of the line equation so we can use one relation to express both circular and linear constraints. This will be important for the generalised procedure.

Clearly, when the joint input is locked, and the platform connections to the other two legs are severed, the

centre point of the R-pair still attached to the platform moves on a line. The platform can rotate about the R-pair centre. This two parameter motion maps to an hyperbolic paraboloid (HP) in the image space. This is verified by transforming the point coordinates $(X : Y : Z)$ in Eq. (5) with Eq. (4), giving the implicit form of the constraint HP:

$$(K_2 - K_1X_3)X_1 - (K_1 + K_2X_3)X_2 + \frac{1}{4}\left[K_3 + 2(K_1x + K_2y)\right]X_3^2 + (K_1y - K_2x)X_3 + \frac{1}{4}\left[K_3 - 2(K_1x + K_2y)\right] = 0.$$

Exploiting some geometric properties of this manifold, we can derive the following parametric form:

$$\begin{bmatrix} X_1 \\ X_2 \\ X_3 \end{bmatrix} = \begin{bmatrix} f(t) + s \\ g(t,s) \\ t \end{bmatrix}, \quad \begin{array}{l} -\infty \le t \le \infty, \\ -\infty \le s \le \infty, \end{array} \tag{7}$$

where

$$f(t) = \frac{(K_3 + 2K_1x + 2K_2y)t^2 + (K_1y - K_2x)4t - 2(K_1x + K_2y) + K_3}{4(K_1t - K_2)},$$
$$g(t,s) = \frac{(K_2 - K_1t)s}{K_1 + K_2t}$$

3. WORKSPACE ANALYSIS

For each leg in the $P\underline{P}R$ platform the active P-pair has a minimum and a maximum extension. Examining Eq. (7), one sees that the only changeable quantities are the length of the P-pair, d_{2_i} and the platform reference point coordinates, $(x : y : z)$; all others are design constants. Hence, for a selected platform reference point there is a minimum and a maximum HP constraint surface corresponding to the minimum and maximum length of d_{2_i}. It turns out that every pair of HP's in a given family have the same curve of intersection because terms dependent on d_{2_i} can be factored out. This can be seen when the intersection curve is projected into the planes $X_1 = 0$, $X_2 = 0$, $X_3 = 0$ and $X_4 = 0$. Therefore, the whole set of HP's in a family forms a pencil of quadrics. The solid bounded by the minimum and maximum HP in each leg is the kinematic image of the platform workspace when the other two legs are disconnected.

The intersection of the three surface bounded solids is the image of the reachable workspace of the entire platform for the selected reference point. The Cartesian reachable workspace is the pre-image obtained by substituting X_1, X_2, X_3 from Eq. 7 into Eq. 4. Note, the platform reference point is completely arbitrary.

For computations, we consider all positions of the platform reference point for fixed platform orientations for each leg. This involves intersecting the constraint solids with the planes X_3 = constant. The reachable workspace for this particular orientation and end-effector reference point is obtained from Eq. 4. The entire reachable workspace is the union of all layers.

4. EXAMPLE

A platform similar to the one shown in Fig. 1 has the geometry listed in Table I. The end-effector reference point is the centroid of the moving triangle. Fig. 2 shows the three constraint solids in the image space. Fig. 3 shows different layers of the reachable Cartesian workspace. There are 13 layers, each representing a 30° increment in the orientation angle. The top layer is for a platform orientation of 180°, the second from the bottom is that of -180°, while the shaded bottom layer is the union of all the layers. The platform has orientation singularities between approximately 10° and 70°, hence the layers representing 30° and 60° are empty. While this indicates the platform design is not good for 360° platform rotations, it is a successful demonstration of the procedure.

Table I
$P\underline{P}R$ platform geometry.

i	$F_{i/\Sigma}$	$M_{i/E}$	ι	$\iota_{1/\Sigma}$	$\iota_{2/1}$
A	$(0:0:1)$	$(-\frac{4}{15}\sqrt{5} : -\frac{2}{15}\sqrt{5} : 1)$	α	0	90°
B	$(3:0:1)$	$(\frac{7}{30}\sqrt{5} : -\frac{2}{15}\sqrt{5} : 1)$	β	90°	90°
C	$(1:3:1)$	$(\frac{\sqrt{5}}{30} : \frac{4}{15}\sqrt{5} : 1)$	γ	225°	90°

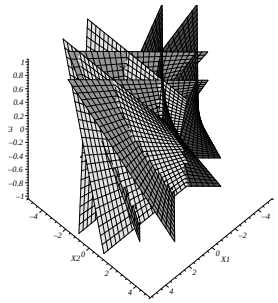

Figure 2. Workspace image.

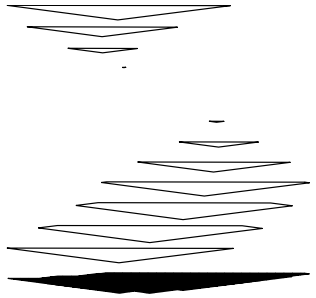

Figure 3. 3D Cartesian layers.

5. CONCLUSIONS AND FUTURE WORK

We have presented the workspace analysis for some PR-type architecturally symmetric platforms, in particular, the $P\underline{P}R$-type, with the aid of kinematic mapping. One of the benefits of the procedure lies in the fact that the Cartesian reachable workspace is dependent on the platform reference point (x, y), which we are free to choose. This makes it easy to compute the different Cartesian workspaces for different reference points. The procedures developed here and in [3], can be combined with those in development to yield an architecture independent procedure. That is, since we are interested in the volume bound by the intersection of solids in the image space, it doesn't matter what the solids look like, as long as we have a parametric representation. Then any three families of any type of constraint surfaces can be intersected. The general procedure would be a tremendous design tool for parallel platforms.

REFERENCES

[1] Bottema, O. and Roth, B., 1979, *Theoretical Kinematics*, Dover Publications, Inc., (1990), New York, N.Y., U.S.A..

[2] Hayes, M.J.D., Husty, M.L., Zsombor-Murray, P.J., 1999, "Kinematic Mapping of Planar Stewart-Gough Platforms", *Proc. 17th Canadian Congress of Applied Mechanics (CANCAM 1999)*, Hamilton, On., Canada, pp. 319-320.

[3] Husty, M.L., 1996, "On The Workspace of Planar Three-legged Platforms", *Proc. World Automation Conf., 6th Int. Symposium on Rob. and Manuf. (ISRAM 1996)*, Montpellier, France, Vol. 3, pp. 339-344.

[4] Merlet, J-P., (1996), "Direct Kinematics of Planar Parallel Manipulators", *IEEE Int. Conf. on Robotics and Automation*, Minneapolis, U.S.A., pp. 3744-3749.